High-Power Rectifier Technologies for Hydrogen Electrolysis

Zhiyu Cao, Peter Wallmeier
AEG Power Solutions GmbH
Emil-Siepmann-Str. 32
Warstein-Belecke, Germany
Tel.: +49 (0)2902 763759
E-Mail: zhiyu.cao@aegps.com, peter.wallmeier@aegps.com
URL: www.aegps.com

Keywords

AC-DC converter, DC power supply, Electrolysis, Active front-end, Vienna rectifier.

Abstract

In this contribution the development of hydrogen electrolysis and its requirements on power supply are reviewed first. To meet these requirements, virous rectifier technologies and devices are developed: primary power control technology for low-voltage high-current application; 2-stage solution consisting of a thyristor-diode front end and an interleaved IGBT chopper for multi-MW application with a DC output voltage up to 1000 V; unidirectional active front end solution with integrated polarization function for application up to 1500 V. All these technologies are verified by type tests and field application (except technology and product under development).

1. Introduction

To achieve climate neutrality the share of renewable energy sources in the power grid is increasing dramatically. Hydrogen electrolysis is one of the major methods to achieve long-term energy storage. Alone with the development of hydrogen electrolysis technologies the technical requirements on the power supply system are changed in last two decades constantly. In this contribution the technical requirements on hydrogen electrolysis power supply are reviewed and discussed first. For low-voltage high-current application the primary power control technology is attractive to achieve high efficiency and small footprint; for the voltage range up to around 1000 V the multi-pulse rectifier in combination with high-current IGBT chopper is a good solution to achieve high efficiency, low total current harmonic distortion (THDi) and high power factor; with increased voltage (i.e. up to 1500 V) the single-stage active front end (AFE) solution becomes more and more attractive. In the following chapters all these technologies will be discussed and verified by type tests and field applications.

2. Review of Technical Requirements on Hydrogen Electrolysis Power Supply

The major technical requirements on hydrogen electrolysis power supply in last two decades are listed in Table I, which can be roughly divided into three phases:

Table I: Technical requirements on hydrogen electrolysis power supply

Grid side requirements | **Year** | **Hydrogen electrolysis side requirements**

Grid	Rsce (example)	Grid code (example)	PF (Typ. req.)	THDi (Typ. req.)	Year	Tech.	Power (Typ. req.)	Voltage (example)	Dynamics	Ripple (Typ. req.)
Transmi-ssion / distribution	High (> 20)	EN61000-2-2 / 12	~ 0.9	~ 10%	00	Alkaline	< 1 MW	50… 250 V	Low	No special requirement
Transmi-ssion / distribution	Medium (10 …20)	TAB 2008	~ 0.95	5%…10%	10	Alkaline / PEM	up to 3 MW+	250… 500 V	Low … Medium	< 5 … 10%
Converter-dominated	Low (<< 10)	VDE-AR-N 4110 / 4120	>0.95 / 0.99 (-1 … 1 ?)	< 3%	20	Alkaline / PEM / solid oxide	up to 20 MW+	500 … 1000V (1500V)	Medium … High	< 3%

(1) in the first decade of this century the installation power of hydrogen electrolysis was marginal. The power grid was typically very strong, and the ratio of grid short-circuit power to hydrogen electrolysis power (R_{sce}) at the power connection point (POC) was relatively high (i.e. $R_{sce} >> 20$). The power quality requirements on the grid side were not so strict like today, for instance only the compliance with EN 61000-2 for low-voltage grid or EN 61000-12 was required. The power factor around 0.9 and the THDi around 10% on full load (FL) were typical requirements. On the electrolysis side the voltage laid typically in a few tens of volts up to approx. 250 V. The power rating was from tens of kW up to hundreds of kW or even up to Megawatt. As systematical studies on the impact of current ripple on the energy consumption and on the degradation of electrolyzers was provided, special requirements on current ripple were not specified.

(2) due to increased share of renewable energy and battery energy storage system (BESS) the grid transmission system operators (TSO) and distribution system operators (DSO) pushed stricter grid compliance requirements constantly. For instance, in Germany the grid connection condition according to TAB2007 and TAB2008 were required for low-voltage and medium-voltage grid, respectively [1]. To comply with these grid codes and to achieve high efficiency and low cost, silicon-controlled rectifier (SCR) solution with different kinds of filter was studied in [2]. On the electrolyzer side, the effect of current ripple on energy consumption was investigated in [3]. A current ripple between 5% to 10% was often specified for the power supply system. To increase electrolysis stack power to Megawatt range, higher number of in series connected cells was applied and the stack voltage increased up to around 500 V.

(3) As results of energy transition the modern converter-dominated power grid has a lower short-circuit power and a higher impedance (weak grid). For reaching a low voltage harmonic distortion, not only the THDi, but also limits of each harmonic current are specified by grid codes. For instance, in VDE-AR-N 4110/4120 R_{sce}-dependent current limits up to 40th harmonics are defined, and a minimum power factor of 0.95 is required from 15% to 100% of full load [4]. Thanks to the rapid development of the high-dynamic proton exchange membrane (PEM) electrolysis technology, parts of the grid frequency regulation function can be taken over by electrolyzers, which requires higher dynamic response on the power supply system. The more recent research works indicate also, the current ripple effects not only on the electrolyzer efficiency, but also has a high impact on the degradation of the electrolyzer membrane [5][6][7]. The power ratting of PEM stacks is increased to over 2 MW, and for alkaline technology the single stack power reaches up to 20 MW. Similar like developments of photovoltaic (PV) inverters and battery energy storage systems (BESS), for reducing current and system-level cost, electrolyzer stack manufacturers and system integrators are pushing the DC voltage toward 1500V.

3. Line-Commutated Primary Power Control

A basic rule for electrical engineer: current costs, voltage does not cost. Hence, for application with low voltage and high current it would be reasonable to control the power on the primary side (high-voltage side). As shown in Fig. 1 the power controller can be implemented by anti-parallel connected thyristors – similar solution like a motor starter. On the secondary side (low-voltage side) of the transformer a standard diode bridge can be applied, which has much lower on-state losses compared to thyristors. By means of this technology higher efficiency and lower cost can be achieved (compared to traditional 6-pulse SCR topology). However, the gird-side performance (i.e. power factor and THDi) can not be improved by this kind of simple primary power control.

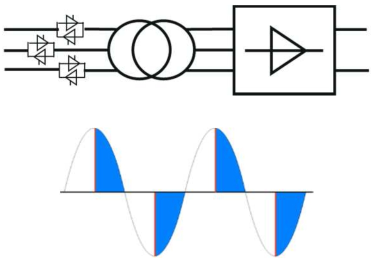

Fig. 1: Primary power controller and the voltage waveform

To reduce the THDi and to enhance the power factor, the voltage sequence control on the transformer primary side can be applied. The basic operation principle is similar like the on-load tab changer (OLTC). Differences are: (a) the tap change is realized by thyristor switches (instead of via mechanical contactors), and (b) periodically tap changing in combination with phase angle control within a grid period. As example the circuit diagram and the voltage waveform of a 48 V / 3000 A rectifier based on the 2-stage primary voltage sequence control is given in Fig. 2.a. In high voltage range the upper switchers (Thyro-P 1 in Fig. 2a) are always operated with full control angle, the output voltage is controlled by changing the firing angle of the bottom switchers (Thyro-P 2 in Fig. 2a). As far as the control angle of the bottom switchers reduced to zero, i.e. in the low voltage rang, the output voltage will be only controlled by the upper switchers and the operation is identical like a simple primary power controller. As listed in Table II, by means of this technology much higher power factors (than the SCR solution) can be achieved.

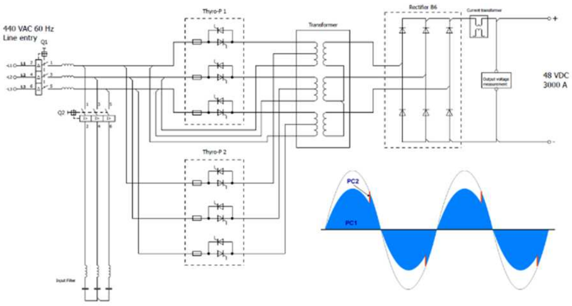

(a)

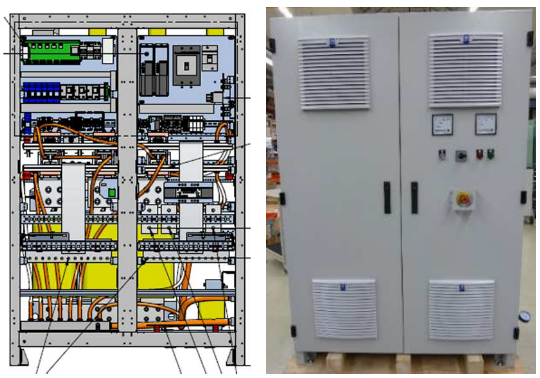

(b)

Fig. 2: Circuit diagram of a 48 V / 3000 A rectifier system with 2-stage voltage sequence control

Table II: Power factor measurement results of the 48 V/ 3000 A rectifier

Vd [V]	Id [A]	PF	Pd [kW]
29,3	1800	0,798	52,7
32,5	2000	0,823	65,0
35,8	2200	0,858	78,7
39,0	2400	0,898	93,7
42,3	2600	0,923	109,9
45,5	2800	0,952	127,5
48,8	3000	0,968	146,3

In Fig. 2.b the mechanical drawing and the photo of the rectifier are given. The cabinet has a dimension of W x D x H = 1050 x 625 x 1800 mm, which represents a power density of 0.22 kW / L and a current density of 2.5 A / L. Obviously, as shown in Fig. 1.b, the 50 Hz transformer is the power density killer.

4. Self-Commutated Primary Power Control

The way to increase power density is to apply self-commutated primary control and to replace the 50 Hz transformer by the medium-frequency (MF) transformer. In Fig. 3 the simplified circuit diagram of the proposed rectifier with self-commutated primary control is illustrated, which is named as matrix rectifier in this paper. The bidirectional switch can be implemented by anti-series connected MOSFETs or IGBTs [8].

In Fig. 4.a the normalized mains voltage waveforms are given. A grid period can be divided into 12 sectors. In each sector we have a highest voltage absolute value (HV), a medium voltage absolute value (MV) and a lowest voltage absolute value (LV), which are changed periodically (Fig. 4.b). As the switching frequency is much higher than the grid frequency (for instance 20 kHz vs. 50 Hz), the grid voltages can be considered constant withing a switching period. If the on-state duty ratio of the bidirectional switches on the phases of MV and LV are proportional to the normalized grid voltage values (Fig. 4.c.), the average absolute voltage on the primary winding of the transformer and the final DC output voltage can be given by (both are normalized values):

$$\begin{aligned} |u_{AB,ave}| &= d_{Mv}(Hv+Mv)+d_{Lv}(Hv+Lv) \\ &= 1.5d, \\ u_{out} &= 1.5\cdot d\cdot n. \end{aligned}$$

Where d denotes the voltage duty ratio of the matrix rectifier and n denotes the voltage ratio of the transformer $n = Ns : Np$.

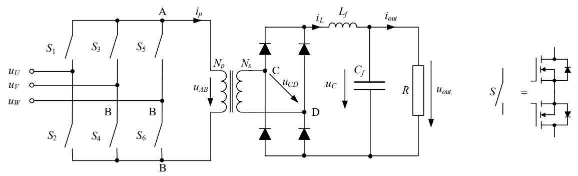

Fig. 3: Simplified circuit diagram of the matrix rectifier

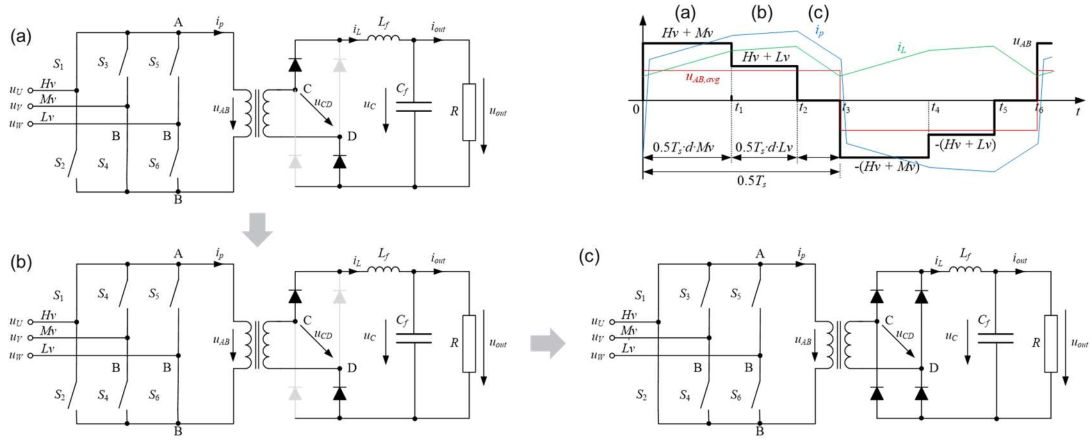

Fig. 5: Voltage and current waveforms and equivalent circuit diagrams within a half switching period

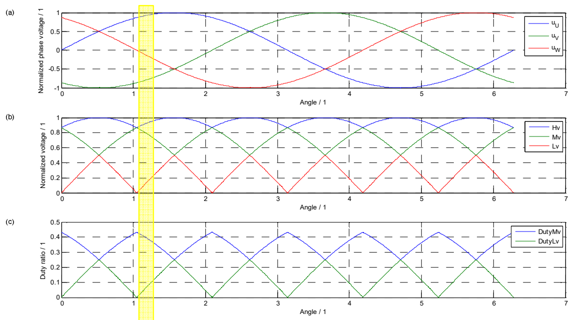

Fig. 4: (a) grid voltage, (b) high-, medium- and low-voltages in each sector, (c) required on-state duty ratio of medium- and low-voltage phase in each sector

The waveforms of the primary voltage u_{AB}, the primary current i_p, the secondary filter choke current i_L are given in Fig. 5. In this sector the voltage on the phase u is positive and highest (Hv); the voltages on phase v and w are negative, and with a medium (Mv) and a lowest (Lv) absolute value, respectively. Within a switching period all phase voltages can be considered as constant. In the time interval (a) S_1 and S_4 are on, the voltage on the primary winding $u_{AB} = Hv + Lv$ with a duration of $0.5 \cdot T_s \cdot d \cdot Mv$; in the time interval (b) S_1 and S_6 are on with a duration of $0.5 \cdot T_s \cdot d \cdot Lv$; in the time interval (c) S_1 and S_2 are on and the primary winding is shorted. By means of this control scheme

- all three phase currents are proportional to phase voltage, which ensures high power factor and low THDi, and
- similar like a buck-type DC-DC converter, the output voltage of the matrix rectifier can be easily control by the duty ratio d.

In Fig. 6 the photo of the matrix rectifier with an output ratting of 60 V / 584 A is given, which reaches a power density of 1 kW / L and a current density of 16.4 A / L.

Fig. 6: Photo of the 60 V / 584 A matrix rectifier (W x D x H = 442 x 456 x 177 mm)

Measurement results at full load (FL) are given in Fig. 7 and Fig. 8. The time-domain current waveforms show a very low current harmonics and a unit power factor. Under part-load condition high power factors and low THDi are achieved (Fig. 9). Bidirectional operation of the matrix rectifier can be also implemented by replacing the diode bridge by MOSFET bridge on die low-voltage side and to operate the rectifier with a special control scheme introduced in [9].

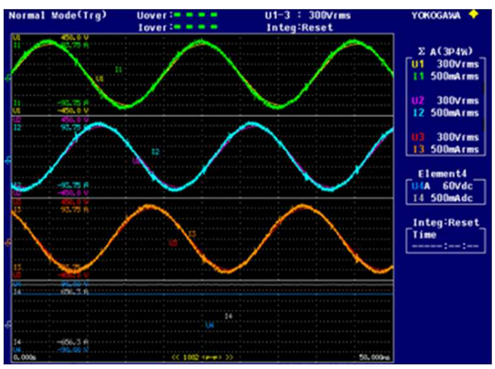

Fig. 7: Measurement results of AC input voltages and currents (100% FL, 60 V / 584 A)

ISBN: 978-9-0758-1542-9 – IEEE: CFP23850-USB

Assigned jointly to the European Power Electronics and Drives Association & the Institute of Electrical and Electronics Engineers (IEEE)

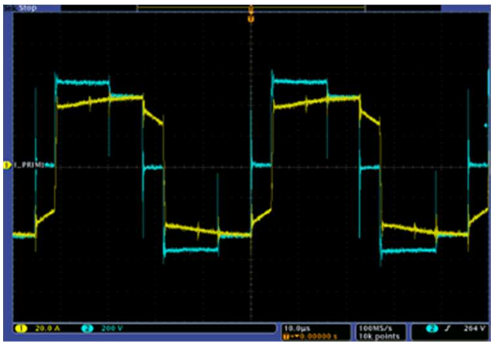

Fig. 8: Measurement result of transformer input voltage and current (100% FL, 60 V / 584 A)

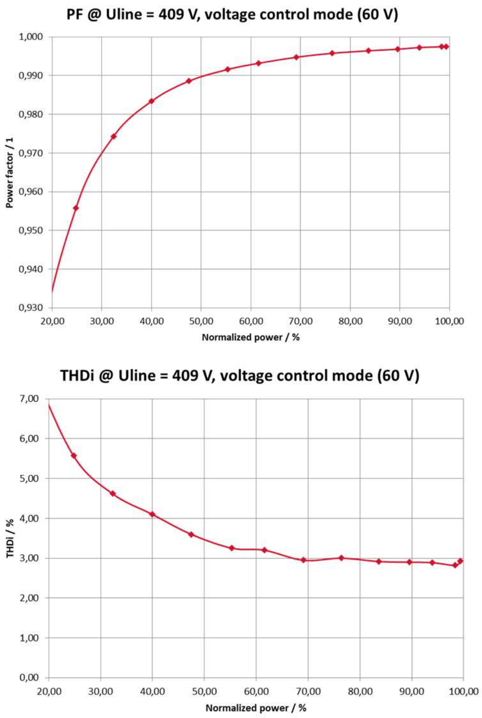

Fig. 9: Power factor and THDi measurements

5. High-Current IGBT Chopper Solution

With increased voltage on electrolysis stacks the primary power control technologies become less attractive. As in mid 2010s the typical power rating went to over 1 Megawatt, connection to medium-voltage grid via MV-transformer is required. Power control in die MV-side is not impossible. For instance, in [2] the modular multilevel converter (MMC) and solid-state transformer (SST) technologies for this application was pre-studied. But with state-of-the-art technologies and components this solution is still not feasible from economical point of view. The traditional SCR technology was still the dominated solution in mid of 2010s thanks the high efficiency, reliability, and low cost. However, as discussed in Chapter 2, due to the enhanced requirements in grid-side power quality and the load-side current ripple, the filtering efforts – both on AC and on DC sides - are very high, which increases the footprint, weight, and cost of the SCR-based power supply system. Customized filter design requires also high engineering cost, product lead time, and project risk.

Hence, a standardized modular solution was desired. The two-stage solution with a thyristor/diode front end and a high-current IGBT chopper became attractive solution [10]. The major characters and advantages of this solution include:

- Standardized power module with 6-pulse diode or thyristor (with full control angular) front end to achieve high reliability
- Interleaved IGBT chopper for voltage regulation and to achieve a very low DC current and voltage ripple (<1%)
- Easy to build a grid-friendly system solution by means of 12, 18, 24, or 36 pulse configurations (only project-specifical transformer required)
- High efficiency (as shown in Fig. 11 and Fig. 12, 98.8% at full load, >99% under part-load condition) and small footprint (W x D x H = 1200 x 600 x 2200 mm for 1.25 MW)
- Low system-level cost: As the DC output voltage is controlled by the IGBT chopper, a relative high DC-link and AC input voltage can be applied, which reduces the cost of AC distribution.

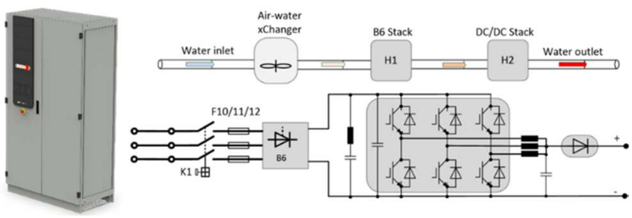

Fig. 10: High-current IGBT chopper rectifier module (1000V / 1250A)

Rectifier output power	1250	kW
Losses into water: 9.14 kW (68%)		
Thyristor	2762	W
IGBT	5379	W
Oring Diode	996	W
Losses into air: 4.33 W (32%)		
DC choke	1798	W
AC choke	993	W
Fuse	482	W
AC contactor	110	W
Cable & busbar (est.)	450	W
Snubber, others (est.)	500	W
Total losses	13.5	kW
Efficiency	98,9%	

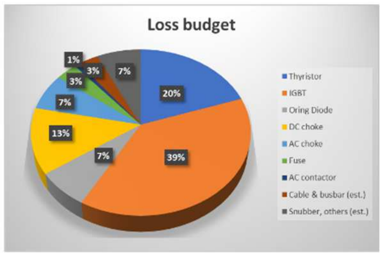

Fig. 11: Calculated of losses budget and efficiency of the chopper module at full load

 ISBN: 978-9-0758-1542-9 – IEEE: CFP23850-USB
Assigned jointly to the European Power Electronics and Drives Association & the Institute of Electrical and Electronics Engineers (IEEE)

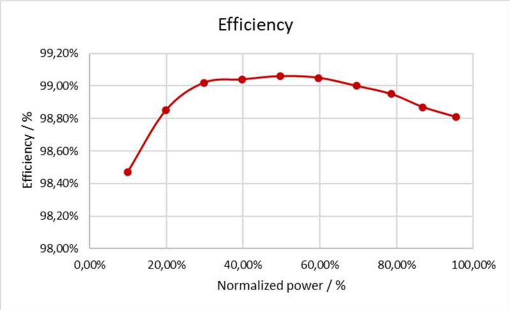

Fig. 12: Results of efficiency measurements of the 1.25 MW IGBT chopper module

With multi-pulse configuration this solution can fulfill most grid code and electrolysis stack requirements. It was successfully applied in lots of electrolysis projects – up to 24 pulse configuration and up to 6.5 MW till now.
As more and more hydrogen electrolysis systems are installed in a converter-dominated grid, where the grid is weak, and the ratio of renewable energy sources and storages is high. In this case TSO-specifical grid code could be required. As an example a hydrogen electrolysis power supply system with a DC output of 900 V / 7200 A is illustrated in Fig. 13, which is connected to a weak grid with R_{sce} ≈ 15. The TSO specifical requirements on harmonic currents (up to 40th harmonics) are shown in Fig. 14 in blue, which are much lower than typical grid code requirements. With 18 pulse configuration the rectifier system reaches a very low THDi = 1.4%, which is much lower than the typical value (around 3%) of AFE rectifiers with IGBT technology. However, currents on 17th, 19th, 35th and 37th harmonics exceed the limits slightly (orange in Fig. 14) . As for this kind of high-power rectifier system an auxiliary power supply winding system is usually required, compensation device can be designed and easily installed at the auxiliary winding. In this project a passive filter consisting of an 850 Hz and a 1750 Hz resonant circuits was designed and installed. The TSO-specifical current harmonics requirements can be fulfilled with the small compensation device (green in Fig. 14).

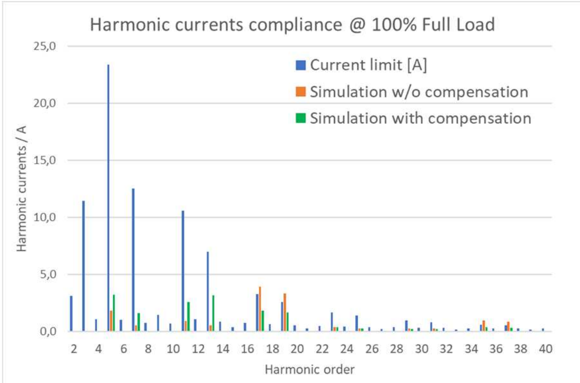

Fig. 14: Verification of TSO-specifical harmonic currents compliance

6. Active Front End (AFE) Solution

In [11] the state-of-the-art three-phase front end topologies are discussed and evaluated (Fig. 15). The line-commutated primary power control discussed in Chapter 3 and the IGBT chopper solution discussed in Chapter 5 belong the buck-type SCR/diode front end; the matrix rectifier introduced in Chapter 4 belongs buck-type AFE solution. As the buck-type AFE is principally a current-source converter, relatively big capacitive

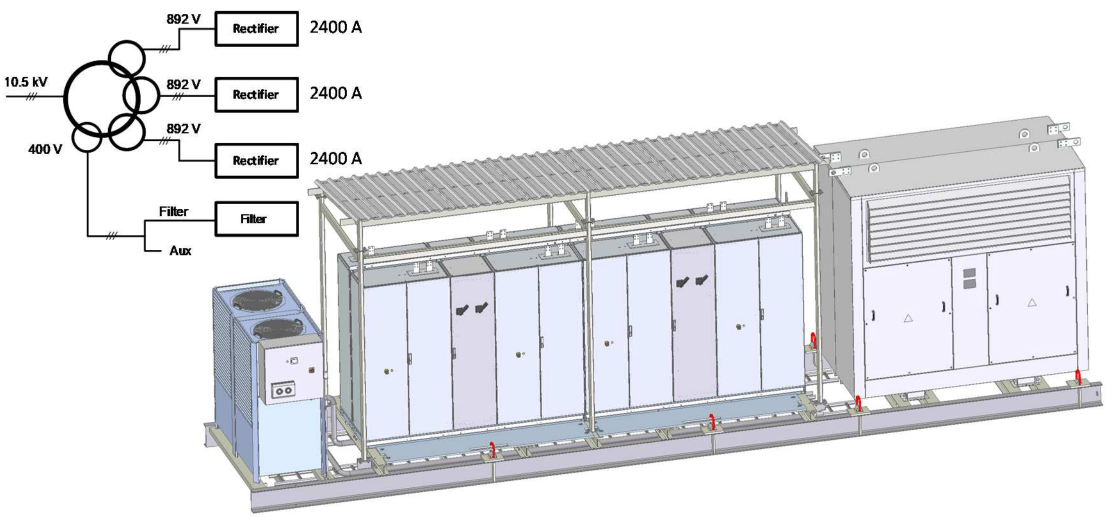

Fig. 13: Hydrogen electrolysis power supply system (900 V / 7200 A) in 18 pulses configuration and IP54 outdoor skid installation

Assigned jointly to the European Power Electronics and Drives Association & the Institute of Electrical and Electronics Engineers (IEEE)

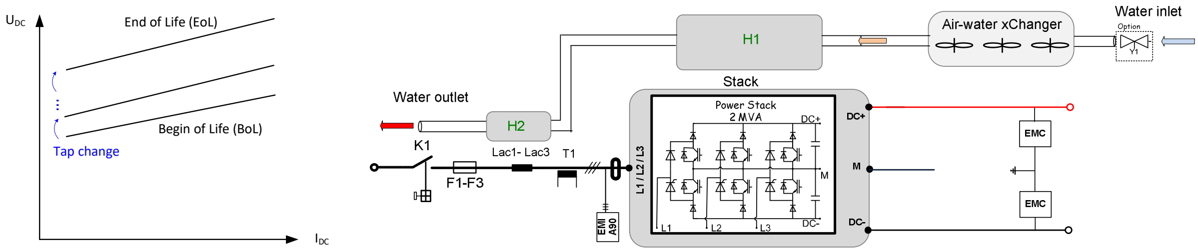

Fig. 16: Operation concept and selected Vienna rectifier topology

filter is required on the grid side, which could results stability issues especially in high power application.

Boost-type AFE is less attractive for hydrogen electrolysis with an end-of-life (EoL) voltage below 1000 V approx., because low AC voltage and high AC current will be required and the cost in in system level will be high. As already mentioned in Chapter 2, for reducing current and cost of power supply system, electrolyzer stack manufacturers and system integrators are pushing the DC voltage toward 1500V by EoL. For this voltage range the boost-type solution becomes interesting again. As the hydrogen application requires only the unidirectional power conversion, the Vienna rectifier topology is selected (Fig. 16). Additional advantageous of this topology for the target application include:

- Grid connection via thyristor / diode: higher reliability and efficiency
- Integrated soft start function
- Provides full current for polarization of electrolyzer stack
- THDi < 3%, power factor > 0.99, and comply with major grid code requirement (i.e. VDE-AR-N 4110/4120 in Germany),

Power module based on the selected Vienna topology with a nominal AC input voltage of 690 V, input current 1800 A and a max. DC output voltage of 1500 V is developed (Fig. 17). To achieve an optimal cost performance ratio, the model-based design and optimization process is applied (Fig. 18.a). Fist, the analytical model for steady-state calculation is developed. Based on the which the steady-state characters incl. component stress, semiconductor losses, choke current ripple etc. are calculated for worst case. The calculated losses budget at rated power (Fig. 18.b) are inputs of thermal calculation of the semiconductor stack and thermal simulation of the cooling plate. The simulated surface temperature of the cooling plate will be feedback for fine-turning the losses and thermal calculation of the semiconductor stack. Final optimization results show the maximum IGBT junction temperature lies slightly below 120°C (Fig. 18.C, vs. maximum 150°C) and the hotspot temperature of the choke lies at 135°C (Fig. 18.d, vs. maximum 155°C for isolation class H). Both with a design margin between 20°C and 30°C.

The product development of the Vienna rectifier is still ongoing. The first lab sample is expected till October of 2023. All technical performances and all calculation and simulation models will be verified by lab sample tests.

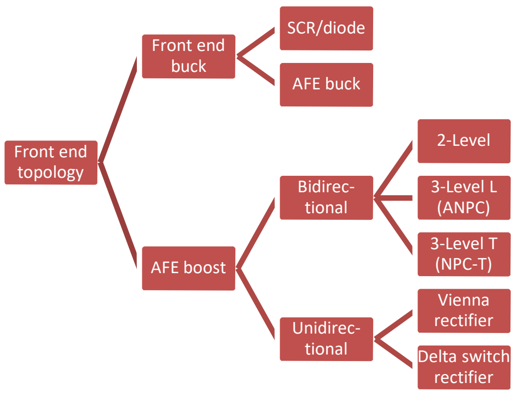

Fig. 15: Front end topologies

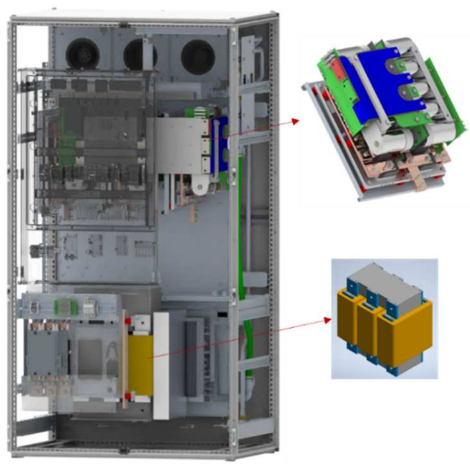

Fig. 17: Mechanical drawing of the Vienna rectifier (690V/1800A/2150kW AC input), up to 1500 V DC output

 ISBN: 978-9-0758-1542-9 – IEEE: CFP23850-USB
Assigned jointly to the European Power Electronics and Drives Association & the Institute of Electrical and Electronics Engineers (IEEE)

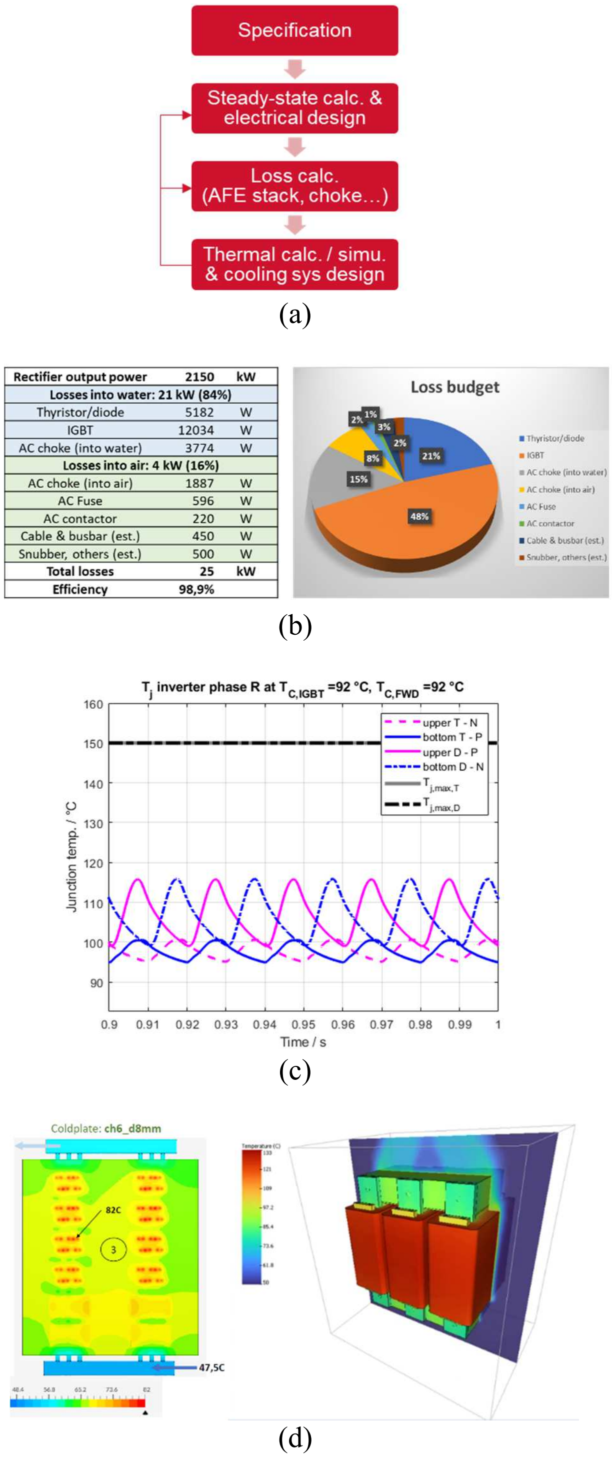

Rectifier output power	2150	kW
Losses into water: 21 kW (84%)		
Thyristor/diode	5182	W
IGBT	12034	W
AC choke (into water)	3774	W
Losses into air: 4 kW (16%)		
AC choke (into air)	1887	W
AC Fuse	596	W
AC contactor	220	W
Cable & busbar (est.)	450	W
Snubber, others (est.)	500	W
Total losses	25	kW
Efficiency	98,9%	

Fig. 18: (a) model-based design and optimization process; (b) loss budget and (c) IGBT junction temperature at full power; (d) thermal simulation results for power stack cooling plate and AC choke

7. Conclusion

In this contribution the development of hydrogen electrolysis and its requirements power supply system in last 2 decades are reviewed. To meeting these requirements, different rectifier technologies are developed and discussed:

- Primary power control technologies are very suitable for low-voltage high-current application.
- The two-stage topology consisting of a thyristor/diode front end and a IGBT chopper is very suitable for multi-MW application with a voltage up to 1000 V.
- For higher EoL voltage up to 1500 V the AFE solution based on Vienna topology becomes attractive.

References

[1] German Association of Energy and Water Industries (BDEW), Technical Conditions for Connection to the low-voltage / medium-voltage network, (TAB 2007 / TAB 2008”), 2007 / 2008

[2] J. Solanki, High Power Factor High-Current Variable-Voltage Rectifiers, PhD thesis, University of Paderborn, 2015

[3] A. Ursúa, et-al, Influence of the power supply on the energy efficiency of an alkaline water electrolyser, International Journal of Hydrogen Energy, Volume 34, Issue 8, 2009, pp 3221-3233

[4] VDE, Technical requirements for the connection and operation of customer installations to the medium-voltage network, November 2018

[5] J. Koponen, V. Ruuskanen, A. Kosonen, M. Niemelä and J. Ahola, "Effect of Converter Topology on the Specific Energy Consumption of Alkaline Water Electrolyzers," in IEEE Transactions on Power Electronics, vol. 34, no. 7, pp. 6171-6182, July 2019, doi: 10.1109/TPEL.2018.2876636.

[6] Parache, F.; Schneider, H.; Turpin, C.; Richet, N.; Debellemanière, O.; Bru, É.; Thieu, A.T.; Bertail, C.; Marot, C. Impact of Power Converter Current Ripple on the Degradation of PEM Electrolyzer Performances. Membranes 2022, 12, 109.

[7] Henning P.C. Buitendach, Rupert Gouws, Christiaan A. Martinson, Carel Minnaar, Dmitri Bessarabov, Effect of a ripple current on the efficiency of a PEM electrolyser, Results in Engineering, Volume 10, 2021

[8] Z. Cao, Converter stage for converting multiple phase alternating current into single phase alternating current and vice versa and method for operating the said converter stage, European Patent EP2993774, 2014

[9] Z. Cao, Bidirectional power converter assembly with potential separation and method for operating the bidirectional power converter circuit, European Patent EP3021475, 2015

[10] Z. Cao, H. Fahnert, J. Schiele, S. Jintendra, N. Fröhleke, J. Böcker, "System Concept and Model-based Optimization of High-Current Variable-Voltage Chopper-Rectifiers," in Proc. of the PCIM Europe Conf., Nurnberg, Germany, 2016

[11] J. W. Kolar and T. Friedli, "The Essence of Three-Phase PFC Rectifier Systems—Part I," in IEEE Transactions on Power Electronics, vol. 28, no. 1, pp. 176-198, Jan. 2013